The Journal of Chemical Physics

Tuning nonequilibrium phase transitions with inertia

Cite as: J. Chem. Phys. **158**, 074904 (2023); https://doi.org/10.1063/5.0138256
Submitted: 09 December 2022 • Accepted: 30 January 2023 • Accepted Manuscript Online: 30 January 2023 • Published Online: 17 February 2023

Ahmad K. Omar, Katherine Klymko, Trevor GrandPre, et al.

View Online Export Citation CrossMark

ARTICLES YOU MAY BE INTERESTED IN

Work statistics in slow thermodynamic processes
The Journal of Chemical Physics **158**, 074104 (2023); https://doi.org/10.1063/5.0138405

Dynamics of chemical reactions on single nanocatalysts with heterogeneous active sites
The Journal of Chemical Physics **158**, 074101 (2023); https://doi.org/10.1063/5.0137751

Phase diagrams—Why they matter and how to predict them
The Journal of Chemical Physics **158**, 030902 (2023); https://doi.org/10.1063/5.0131028

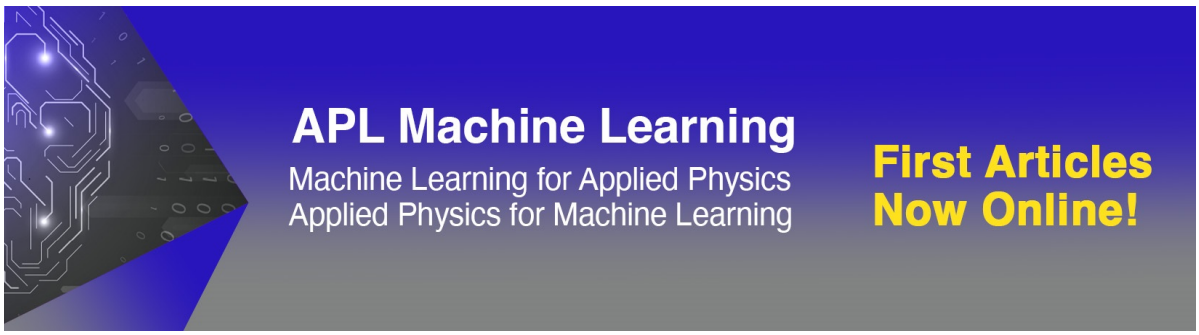

AIP Publishing

© 2023 Author(s).

The Journal of Chemical Physics ARTICLE scitation.org/journal/jcp

Tuning nonequilibrium phase transitions with inertia

Cite as: J. Chem. Phys. 158, 074904 (2023); doi: 10.1063/5.0138256
Submitted: 9 December 2022 • Accepted: 30 January 2023 •
Published Online: 17 February 2023

View Online Export Citation CrossMark

Ahmad K. Omar,[1,2,a] Katherine Klymko,[3,4,b] Trevor GrandPre,[5] Phillip L. Geissler,[6,7] and John F. Brady[8]

AFFILIATIONS

[1] Department of Materials Science and Engineering, University of California, Berkeley, California 94720, USA
[2] Materials Sciences Division, Lawrence Berkeley National Laboratory, Berkeley, California 94720, USA
[3] NERSC, Lawrence Berkeley National Laboratory, Berkeley, California 94720, USA
[4] Computational Research Division, Lawrence Berkeley National Laboratory, Berkeley, California 94720, USA
[5] Department of Physics, University of California, Berkeley, California 94720, USA
[6] Department of Chemistry, University of California, Berkeley, California 94720, USA
[7] Chemical Sciences Division, Lawrence Berkeley National Laboratory, Berkeley, California 94720, USA
[8] Division of Chemistry and Chemical Engineering, California Institute of Technology, Pasadena, California 91125, USA

[a] **Author to whom correspondence should be addressed:** aomar@berkeley.edu
[b] kklymko@lbl.gov

ABSTRACT

In striking contrast to equilibrium systems, inertia can profoundly alter the structure of active systems. Here, we demonstrate that driven systems can exhibit effective equilibrium-like states with increasing particle inertia, despite rigorously violating the fluctuation–dissipation theorem. Increasing inertia progressively eliminates motility-induced phase separation and restores equilibrium crystallization for active Brownian spheres. This effect appears to be general for a wide class of active systems, including those driven by deterministic time-dependent external fields, whose nonequilibrium patterns ultimately disappear with increasing inertia. The path to this effective equilibrium limit can be complex, with finite inertia sometimes acting to accentuate nonequilibrium transitions. The restoration of near equilibrium statistics can be understood through the conversion of active momentum sources to passive-like stresses. Unlike truly equilibrium systems, the effective temperature is now density dependent, the only remnant of the nonequilibrium dynamics. This density-dependent temperature can in principle introduce departures from equilibrium expectations, particularly in response to strong gradients. Our results provide additional insight into the effective temperature ansatz while revealing a mechanism to tune nonequilibrium phase transitions.

Published under an exclusive license by AIP Publishing. https://doi.org/10.1063/5.0138256

INTRODUCTION

Particle dynamics that break time-reversal symmetry result in a non-Boltzmann distribution of microstates, leading to phase transitions and pattern formation that defy equilibrium intuition. Self-propelled particles can phase separate in the absence of cohesive interactions, a phenomenon commonly referred to as motility-induced phase separation (MIPS).[1–4] Externally manipulating the trajectories of particles (e.g., with magnetic or electric fields) can result in microphases and pattern formation[5–10] despite purely repulsive, simple interaction potentials. While the observation of these and numerous other nonequilibrium phase transitions in natural and synthetic systems is now routine, the theoretical description of these transitions is clouded by the absence of *a priori* knowledge of the distribution of microstates.

Understanding the many-body phase behavior of driven systems remains a principal challenge in nonequilibrium statistical mechanics. However, it has become clear that some nonequilibrium systems may admit an *effective* Boltzmann distribution of states, a feature that radically improves our ability to understand these systems.[11] Athermal granular materials have been described by the Edwards ensemble, which, in simple terms, is a statistical

Published under an exclusive license by AIP Publishing

mechanical framework based on the assertion that states with equal volume (rather than energy) have equal probability.[12,13] The fluctuations of boundary-driven arrested materials have also been posited to be controlled by an effective temperature (albeit, not uniquely defined).[14,15]

In the case of active or locally driven matter—where the breaking of time-reversal symmetry is due to a particle-level driving force—effective equilibrium states have been invoked to explain emergent structural features and phase transitions with varying degrees of success.[8,16–23] In these scenarios, energy scales born from the active dynamics (which can be defined using, e.g., linear response theory or invoking Stokes–Einstein relations) play the role of an effective temperature that is then used to map these driven systems onto an equilibrium analog.[24–33] However, assessing the success of effective temperature ideas to describe nonequilibrium steady states remains largely empirical. Recent work by O'Bryne and Tailleur demonstrated that the dynamics of tactic active matter can be rigorously mapped to effective passive systems at a hydrodynamic level.[34,35] On a microscopic level, active forces under certain limits can act as traditional thermal forces by satisfying an effective fluctuation–dissipation theorem (FDT).[36,37] However, the general question remains: When can nonequilibrium systems be rigorously mapped to effective equilibrium states?

In this article, we explore the question raised above in the context of active systems. Despite the presence of active forces that strictly violate the FDT on a microscopic level, we demonstrate a new limit in which nominally nonequilibrium systems can be pushed to effective equilibrium states simply by increasing inertia. This limit occurs when the translational momentum relaxation time τ_M is much larger than the intrinsic timescale associated with translational active forces τ_A as measured through the Stokes number $\mathrm{St} \equiv \tau_M/\tau_A$. When $\mathrm{St} \to \infty$, active forces behave as thermal forces with the kinetic temperature playing the role of a now *density-dependent* effective temperature. We show that a variety of nonequilibrium transitions observed in the overdamped limit are attenuated with increasing inertia while equilibrium-like transitions are restored. Our results offer a new interpretation for the reported[39–43] dependency of nonequilibrium phase transitions on translational inertia and further insight into the applicability of the effective temperature perspective.

MANY-BODY PHASE BEHAVIOR

While the impact of inertia on active dynamics has been recently investigated,[39,41–56] a generalized understanding of its impact on active phase behavior has remained elusive. Before proceeding to demonstrate the impact of inertia on the many-body phase behavior of driven systems, we briefly discuss the model systems and their known equilibrium limit. We consider the microscopic distribution of the positions $\mathbf{x}^N$ of N particles each with mass m and each experiencing conservative interparticle/external forces $\mathbf{F}^{\mathrm{C}} = \mathbf{F}^{\mathrm{int}} + \mathbf{F}^{\mathrm{ext}} = -\nabla V(\mathbf{x}^N)$ (where V is the potential) and two nonconservative forces: a drag force $\mathbf{F}^{\mathrm{drag}}$ that dissipates the particle's energy and a fluctuating source force $\mathbf{F}^{\mathrm{source}}$ that injects energy into the system. The FDT establishes the relationship between the fluctuating and dissipative forces that is required to rigorously recover a Boltzmann distribution of microstates $\mathcal{P}(\mathbf{x}^N) \propto \exp[-V(\mathbf{x}^N)/k_BT]$, where k_BT is the energy scale associated with the source. Taking the drag coefficient of each particle to be independent, memoryless, and constant (i.e., $\mathbf{F}^{\mathrm{drag}} = -\zeta\mathbf{u}$, where ζ is the drag coefficient and $\mathbf{u}$ is the particle velocity), the FDT constrains the source force to have a mean of $\mathbf{0}$ and a variance of $\langle \mathbf{F}^{\mathrm{source}}(t)\mathbf{F}^{\mathrm{source}}(t')\rangle = 2k_BT\zeta\delta(t-t')\mathbf{I}$.

Nonequilibrium forces can satisfy the FDT in certain limits, making the notion of an effective temperature exact under these conditions. For instance, for active Brownian particles (ABPs), the source of fluctuations is $\mathbf{F}^{\mathrm{source}} = \mathbf{F}^{\mathrm{act}} = \zeta U_0\mathbf{q}$, where U_0 is the intrinsic active speed and $\mathbf{q}$ is the particle orientation. Taking the dynamics of $\mathbf{q}$ to be diffusive and overdamped with rotary diffusion constant D_R, the particles move persistently for a characteristic timescale $\tau_R = D_R^{-1}$. Rotational inertia can profoundly alter the dynamics of ABPs (see the recent work of Sandoval[49]); however, we neglect such effects here to simplify our analysis and isolate the role of translational inertia on systems with translational active forces. While generally not satisfying the FDT, $\mathbf{F}^{\mathrm{act}}$ does so in the limit that $\tau_R \to 0$ (i.e., $\langle \mathbf{F}^{\mathrm{act}}(t)\mathbf{F}^{\mathrm{act}}(t')\rangle = 2k_BT^{\mathrm{eff}}\zeta\delta(t-t')\mathbf{I}$) with an effective temperature of $k_BT^{\mathrm{eff}} = \zeta D^{\mathrm{act}}$ where $D^{\mathrm{act}} = \frac{U_0^2\tau_R}{d(d-1)}$ is the intrinsic active diffusion constant in d spatial dimensions.[37,38] This is often the limit explored in experiments that have observed effective Boltzmann distributions in active systems.[25,31]

Short of this limit, with the microscopic dynamics in strict violation of the FDT, we now demonstrate the implications of inertia on the phase behavior of active systems. We conduct simulations[57,58] (see the supplementary material for details) of effective hard-sphere ABPs in three dimensions (3D), the phase behavior of which has been recently established.[23,38] In the overdamped hard-sphere limit, the phase diagram is characterized by two geometric parameters: the ratio of the run length $\ell_0 \equiv U_0\tau_R$ to particle diameter σ and the volume fraction ϕ. Here, the system undergoes MIPS for a broad range of ℓ_0/σ and ϕ.[38] The addition of translational inertia adds a third dimensionless axis to the phase diagram, quantified by $\mathrm{St} \equiv \tau_M/\tau_A \equiv (m/\zeta)/\tau_R$. Selecting a state well within the regime of MIPS such that the liquid and gas densities are appreciably distinct, we observe [see Fig. 1(a)] a rapid and monotonic elimination of coexistence with increasing St and the absence of MIPS entirely when $\mathrm{St} > 0.03$.

The sensitivity of MIPS to inertia in 2D was first reported by Mandal *et al.*[39] who demonstrated that, for all values of ℓ_0/σ and for high enough St, a homogeneous state was observed *in lieu* of MIPS. As we later argue, the absence of MIPS with increasing inertia is rooted in the system reaching an effective equilibrium state. If this is indeed the case, we should additionally observe the restoration of equilibrium transitions. In the case of our hard-sphere system, Boltzmann statistics would result in the equilibrium freezing transition with coexisting fluid and solid densities[59,60] of $\phi_{\mathrm{fluid}} = 0.494$ and $\phi_{\mathrm{solid}} = 0.545$. Importantly, equilibrium freezing is athermal in origin and thus does not depend on the precise value of k_BT^{eff}.

In the overdamped limit, activity dramatically shifts the freezing transition toward higher densities[38] with the solid phase exhibiting a nearly close-packed density ($\phi_{\mathrm{solid}} \to 0.74$) for activities as small as $\ell_0/\sigma = 5.0$ [see $\mathrm{St} = 0$ in Fig. 1(b)]. In the limit of small run lengths $\ell_0/\sigma \to 0$ where the FDT is satisfied, it was recently shown that, despite the use of a continuous potential, athermal active particles display a freezing transition that closely resembles that of equilibrium hard spheres.[38] Departing from the overdamped limit, we observe a shift in the crystal coexistence region to lower

Published under an exclusive license by AIP Publishing

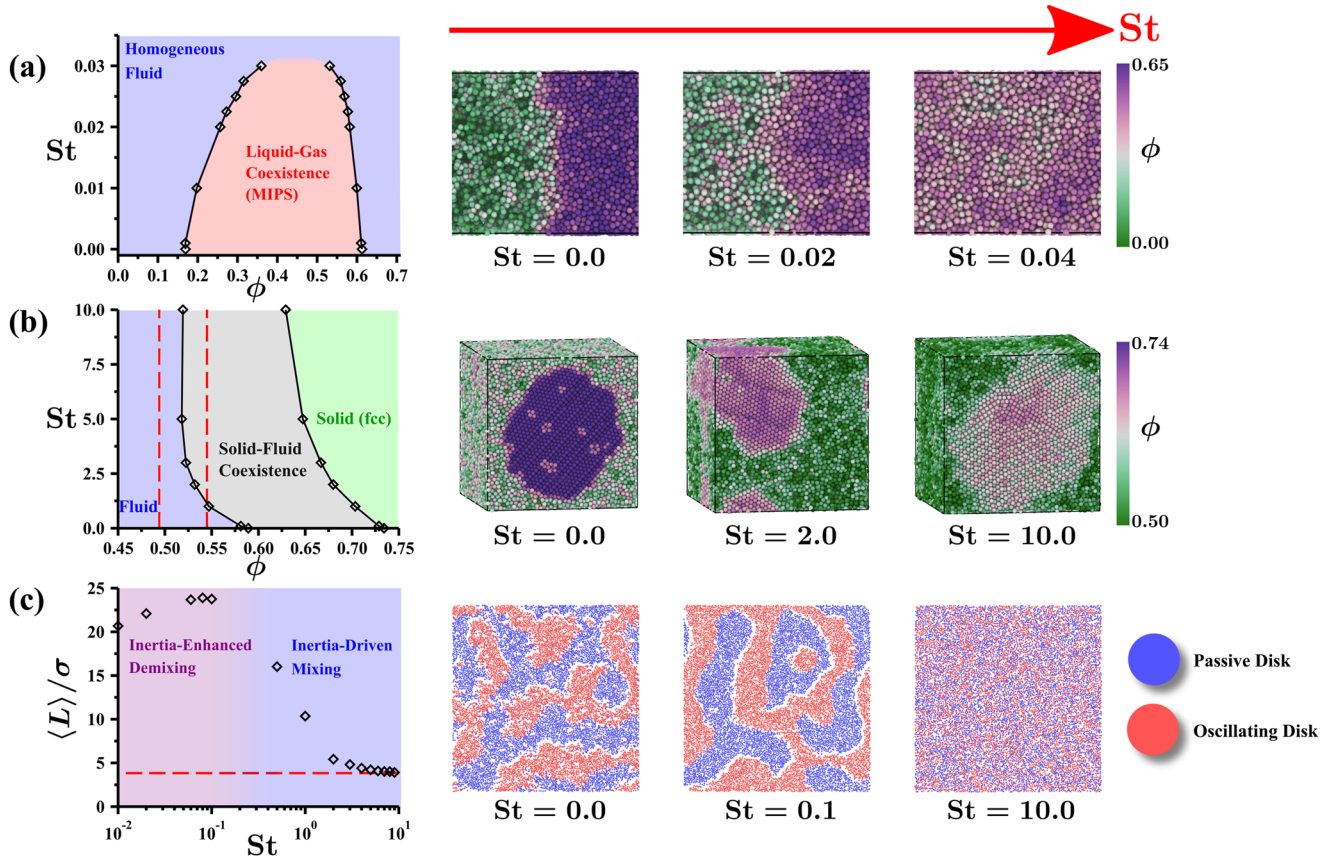

FIG. 1. Inertia dependence of (a) MIPS ($\ell_0/\sigma = 50.0$) and (b) crystallization ($\ell_0/\sigma = 5.0$) of active Brownian spheres (see Ref. 38 for St = 0 phase diagram) and (c) pattern formation in a 50 : 50 mixture (with number density $\rho\sigma^2 = 0.45$) of oscillating ($U_0\sigma/D^B = 70$, $\ell_0/\sigma \equiv U_0/\omega = 1.67$) and passive soft disks (see Ref. 9 for St = 0 phase diagram). Dashed lines denote equilibrium expectations.

densities [see Fig. 1(b)], consistent with our expectations of a return to an effective equilibrium. We note that the crystallization transition appears to be much less sensitive to inertia than MIPS, with the coexistence window continuing to shift to lower densities for St > 1. For St > 5, the densities (particularly that of the fluid) appear to saturate at values that, while significantly closer, are decidedly distinct from the expected values of equilibrium freezing. The source of this discrepancy is possibly rooted in the nonequilibrium origins of the effective temperature, which we later show manifest in its *density dependence*.

Thus far, increasing inertia has monotonically pushed the phase behavior of active systems to more closely resemble effective equilibrium systems. However, it should be emphasized that reaching the effective equilibrium appears to occur in the asymptotic limit of high inertia. Intermediate values of inertia can also *heighten* the nonequilibrium features observed in overdamped phase transitions. 2D systems of repulsive active–passive mixtures are known to form microphases when the source of activity is an oscillatory deterministic force [$\mathbf{F}^{\text{act}} = \zeta U_0 \mathbf{q}$ with $\mathbf{q}(t) = \sin(\omega t)\hat{\mathbf{e}}_{\mathbf{x}} + \cos(\omega t)\hat{\mathbf{e}}_{\mathbf{y}}$].[8,9] Here, all particles experience Brownian forces $\mathbf{F}^{\mathbf{B}}$ (resulting in a translational diffusivity $D^B \equiv k_B T/\zeta$) that do satisfy the FDT (i.e., $\mathbf{F}^{\text{source}} = \mathbf{F}^{\mathbf{B}}$ and $\mathbf{F}^{\text{source}} = \mathbf{F}^{\text{act}} + \mathbf{F}^{\mathbf{B}}$ for the passive and active particles, respectively). By introducing translational inertia with $\text{St} \equiv \tau_M/\tau_A \equiv (m/\zeta)\omega$, we observe [see Fig. 1(c)] an enhancement in the average size $\langle L \rangle$ of the microdomains (and interfacial smoothness) with increasing inertia before eventually reaching the effective equilibrium limit. That there exists an optimum St for accentuating nonequilibrium transitions makes clear the path toward effective equilibrium can be complex.

THEORY AND DISCUSSION

We now explore the origins of the apparent return to equilibrium phase behavior of active systems with increasing inertia. Before proceeding to interacting systems, it is instructive to consider the distribution of ideal ABPs ($\mathbf{F}^{\text{int}} = \mathbf{0}$), which in addition to the active force, also experience translational Brownian forces $\mathbf{F}^{\mathbf{B}}$. These dynamics result in a Fokker–Planck equation for the probability density $\mathcal{P}(\mathbf{x}, \mathbf{u}, \mathbf{q}, t)$,[61]

$$\frac{\partial \mathcal{P}}{\partial t} = -\nabla_{\mathbf{x}} \cdot \mathbf{j}^{\mathbf{x}} - \nabla_{\mathbf{u}} \cdot \mathbf{j}^{\mathbf{u}} - \nabla_{\mathbf{q}} \cdot \mathbf{j}^{\mathbf{q}}, \tag{1}$$

Published under an exclusive license by AIP Publishing

where $\mathbf{j}^{\psi}$ and ∇_{ψ} are the flux of probability and gradient operator in ψ-space, respectively (see the supplementary material).

By taking statistical moments (see the supplementary material) of Eq. (1) in both $\mathbf{u}$ and $\mathbf{q}$, one finds that the steady-state number density field $\rho(\mathbf{x}) = \int \mathcal{P}\, d\mathbf{u}\, d\mathbf{q}$ of ideal ABPs satisfies mass conservation $\nabla_{\mathbf{x}} \cdot \mathbf{j}^{\rho} = 0$, where the density flux $\mathbf{j}^{\rho}$ can be determined from linear momentum conservation,

$$\nabla_{\mathbf{x}} \cdot \underbrace{\boldsymbol{\sigma}}_{\substack{\text{particle}\\ \text{stress}}} + \underbrace{\zeta U_0 \mathbf{m}}_{\substack{\text{active body}\\ \text{force}}} + \underbrace{\rho \mathbf{F}^{\text{ext}}}_{\substack{\text{external}\\ \text{body force}}} - \underbrace{\zeta \mathbf{j}^{\rho}}_{\substack{\text{drag body}\\ \text{force}}} = \mathbf{0}, \tag{2}$$

where $\mathbf{m}(\mathbf{x}) = \int \mathcal{P}\, \mathbf{q}\, d\mathbf{u}\, d\mathbf{q}$ is the polarization density of the particles. For ideal ABPs, the stress is simply the kinetic stress $\boldsymbol{\sigma} = \boldsymbol{\sigma}^{K} = -\rho m \langle \mathbf{uu} \rangle$. The nonconservative and external forces act as body forces—sources or sinks of momentum that can generate stress gradients in a system. The active body force[62–66] injects momentum into the system through the polarization field, which, at steady state, satisfies $\mathbf{m} = -\frac{\tau_R}{d-1} \nabla_{\mathbf{x}} \cdot \mathbf{j}^{\mathbf{m}}$. An active (or "swim") stress[67–71] is often defined $\boldsymbol{\sigma}^{\text{act}} = -\frac{\zeta U_0 \tau_R}{d-1} \mathbf{j}^{\mathbf{m}} = -\frac{\zeta U_0 \tau_R}{d-1} \rho \langle \mathbf{uq} \rangle \sim \tau_R \rho \langle \mathbf{u} \mathbf{F}^{\text{act}} \rangle$, allowing Eq. (2) to be expressed as $\nabla_{\mathbf{x}} \cdot (\boldsymbol{\sigma} + \boldsymbol{\sigma}^{\mathbf{act}}) + \rho \mathbf{F}^{\text{ext}} - \zeta \mathbf{j}^{\rho} = \mathbf{0}$.[65] While derived here for ideal systems, Eq. (2) is also general to interacting ABPs,[64,72] which generate an additional stress $\boldsymbol{\sigma}^{\mathbf{int}} = -\rho \langle \mathbf{x} \mathbf{F}^{\mathbf{int}} \rangle$.

We can now approximate the steady-state distribution of ideal ABPs as a function of $\text{St} \equiv (m/\zeta)/\tau_R$. In the presence of an infinite planar hard (no flux) wall at $z = 0$ with a bulk density of ρ^{∞} as $z \to \infty$, ideal passive systems would recover a uniform density field $\rho(z) = \rho^{\infty}$, consistent with Boltzmann statistics. In contrast, overdamped ABPs strongly accumulate on no-flux boundaries despite the absence of an energetic driving force for wetting the surface.[62] Continuing to take statistical moments of $\mathcal{P}(\mathbf{x}, \mathbf{u}, \mathbf{q})$ and closing at the nematic level (see the supplementary material for a complete derivation), for $d = 2$ we find a density profile of

$$\rho(z) = \rho^{\infty} \left(1 + \frac{D^{\text{act}}}{D^B (1 + \text{St})} \exp[-z\lambda] \right) \tag{3}$$

and a polarization density of

$$\mathrm{m}_z(z) = -\frac{\alpha \lambda D^B}{U_0} \frac{\rho^{\infty} D^{\text{act}}}{\beta (D^B + D^{\text{act}}) - D^{\text{act}}} \exp[-z\lambda], \tag{4}$$

where λ is the inertia-dependent inverse screening length,

$$\lambda^2 = \frac{(d-1)\beta (1 + D^{\text{act}}/D^B)}{(\alpha \gamma \delta^2)},$$

where $\delta = \sqrt{\tau_R D^B}$ is a microscopic length and we have defined the following dimensionless variables:

$$\alpha = 1 + \frac{D^{\text{act}}}{D^B} \left(\frac{\text{St}}{1 + \text{St}} \right),$$

$$\beta = 1 + (d-1)\text{St},$$

$$\gamma = \frac{1}{1 + \text{St}} \left(1 + \frac{D^{\text{act}}}{D^B} \frac{(d-1)\text{St}}{2} \right).$$

For $\text{St} = 0$, our results exactly capture the overdamped limit[62] while for increasing St we observe a reduction in the degree of accumulation [see Fig. 2(a)] that is consistent with simulation. These trends continue until achieving a uniform distribution of particles as $\text{St} \to \infty$, consistent with equilibrium expectations.

The origins of this apparent effective equilibrium can be understood in the context of linear momentum conservation, which governs the dynamics of the density field. With increasing St, the decorrelation of active force and particle velocity diminishes the active stress $\boldsymbol{\sigma}^{\mathbf{act}} \sim \langle \mathbf{u} \mathbf{F}^{\text{act}} \rangle$ while the kinetic stress grows and increasingly resembles that of a passive system (i.e., $\boldsymbol{\sigma}^{K} \to -\rho k_B T^{\text{eff}} \mathbf{I}$ as $\text{St} \to \infty$, see the supplementary material). As a result, the steady-state momentum balance Eq. (2) becomes indistinguishable

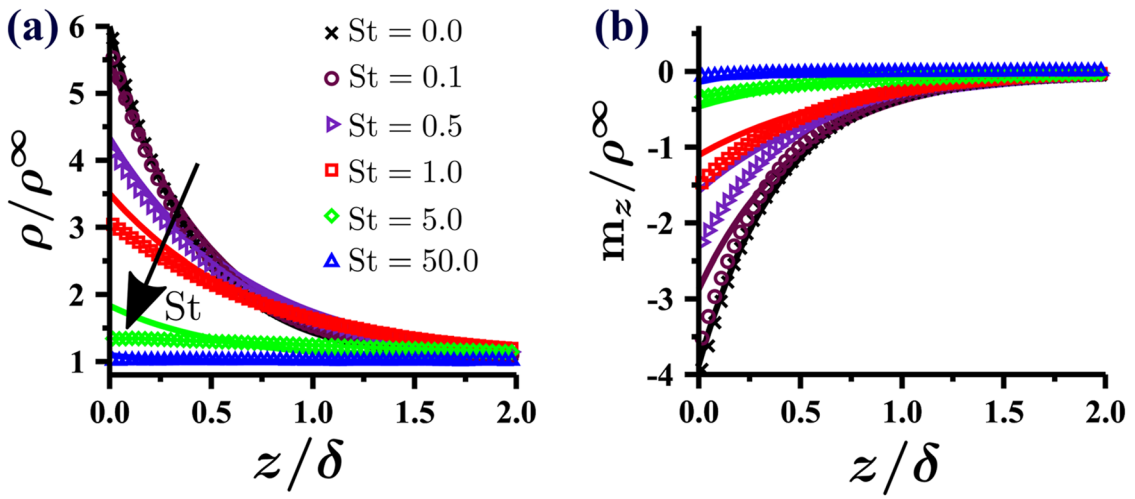

FIG. 2. Simulation (symbols) and theoretical (lines) results of (a) ρ and (b) m_z [Eq. (4)] for ideal ABPs with $D^{\text{act}}/D^B = 5.0$ near a no-flux boundary.

Published under an exclusive license by AIP Publishing

from that of a passive system, resulting in a Boltzmann distribution with an effective temperature given by the kinetic temperature $k_B T^{\text{eff}} \equiv m\langle \mathbf{u}\cdot\mathbf{u}\rangle/d = \zeta\left(D^B + D^{\text{act}}\right)$ (see the supplementary material).

This exchange of active stress for kinetic stress (and the indistinguishably of the kinetic stress to that of a passive system) with increasing inertia, in essence, renders activity as nothing more than an energy reservoir, much like a thermal bath. This stress exchange is general to interacting active systems, and it is in fact a consequence of the first law, which takes the form (on a per-particle basis and using the Stratonovich convention) $d\mathcal{H} = m\mathbf{u}\cdot d\mathbf{u} - \mathbf{F}^{\mathbf{C}}\cdot d\mathbf{x}$. At steady state, the absence of average energy production results in $\frac{d}{dt}\langle\mathcal{H}\rangle = \langle \mathbf{u}\cdot(m\dot{\mathbf{u}} - \mathbf{F}^{\mathbf{C}})\rangle = 0$. Using this and our equation of motion $m\dot{\mathbf{u}} = \mathbf{F}^{\mathbf{C}} + \mathbf{F}^{\text{source}} + \mathbf{F}^{\text{drag}}$ leads to

$$\underbrace{\langle -\zeta \mathbf{u}\cdot\mathbf{u}\rangle}_{\substack{\text{dissipation}\\ \text{rate, } \dot{q}}} + \underbrace{\langle \mathbf{u}\cdot\mathbf{F}^{\text{act}}\rangle}_{\substack{\text{active work}\\ \text{rate, } \dot{w}^{\text{act}}}} = 0, \tag{5}$$

irrespective of whether $\mathbf{F}^{\mathbf{B}}$ is included in $\mathbf{F}^{\text{source}}$. Equation (5) simply states that the rate of active work production is balanced by the rate of dissipation[36,37,73–79] and provides a relation between velocity–velocity and orientation–velocity correlations with deep mechanical implications. For homogeneous and isotropic systems, this can be appreciated by taking the ratio of the kinetic pressure $P^K = -\text{tr}(\boldsymbol{\sigma}^K)/d = \rho m\langle \mathbf{u}\cdot\mathbf{u}\rangle/d$ to the active pressure $P^{\text{act}} = -\text{tr}(\boldsymbol{\sigma}^{\text{act}})/d = \frac{\tau_R}{d(d-1)}\rho\langle \mathbf{u}\cdot\mathbf{F}^{\text{act}}\rangle$, which, using Eq. (5), must result in $P^K/P^{\text{act}} = (d-1)\text{St}$. Figure 3(a) confirms this result for interacting ABPs—active stress must be reduced in exchange for kinetic stress with St.

Two crucial questions remain for interacting active systems: As $\text{St}\to\infty$, (i) does the kinetic temperature also play the role of an effective equilibrium temperature and (ii) does the interaction stress $\boldsymbol{\sigma}^{\text{int}}$ resemble that of passive systems at this temperature? Fig. 3(b) demonstrates that the kinetic temperature of homogeneous fluids of active Brownian spheres exhibits strong dependencies on density, reaching the ideal limit $k_B T^{\text{eff}} \to \zeta D^{\text{act}}$ only as $\phi\to 0$ and $\text{St}\to\infty$. Upon normalizing the interaction pressure $P^{\text{int}} = -\text{tr}(\boldsymbol{\sigma}^{\text{int}})/d$ by the density-dependent kinetic temperature, we indeed observe a return to the equilibrium hard-sphere equation of state with increasing St for all ϕ as shown in Fig. 3(c). Such a collapse would not have been possible if a density-independent energy scale had been selected and indirectly reflects the elimination of the uniquely active contributions to $\boldsymbol{\sigma}^{\text{int}}$ with St.

Physically, the origin of this equilibrium-like distribution and distinctly nonequilibrium density-dependent effective temperature can be understood by considering the various timescales present in the system. In addition to the momentum relaxation time τ_M and active reorientation time τ_R, there is a timescale associated with interactions, τ_{int}. This timescale could, for example, be the characteristic time between hard-sphere collisions. In the limit $\text{St}\to\infty$, $\tau_M \gg \tau_R$ and the particle orientation—the distinguishing feature of active matter—ceases to play any dynamical role in the system. However, if $\tau_R > \tau_{\text{int}}$, the FDT (which requires τ_R to be much smaller than *all* other timescales) remains unsatisfied. The active force acts as a source of kinetic energy, but it requires unimpeded particle motion for a duration of τ_R to generate a kinetic energy of ζD^{act}. Collisions occurring on timescales faster than the active timescale (i.e., $\tau_R \gg \tau_{\text{int}}$) thus reduce the kinetic energy generated by the active force. The increased collision rate with ϕ is precisely why the effective temperature decreases with concentration.

The dependence of $k_B T^{\text{eff}}$ on ϕ suggests a coupling between temperature and local density[1,8,80] that distinguishes $\text{St}\to\infty$ from a true equilibrium limit. Such a dependence may, in principle, even generate unique density fluctuations and phase transitions. It is likely that this coupling alters the crystallization phase boundaries [cf. Fig. 1(b)] from reaching the known equilibrium values as the two phases necessarily coexist *at different effective temperatures*. This result suggests that while for *spatially homogeneous* systems, inertial active matter may strongly resemble systems in thermodynamic equilibrium, situations in which strong density gradients arise (as in the case of crystallization or the presence of a strong external potential) will result in departures from equilibrium expectations. Moreover, it is likely that even in scenarios of spatial homogeneity, the density dependence of the effective temperatures alters the distribution of local density fluctuations from equilibrium expectations. While this is the subject of future investigation, it is likely that

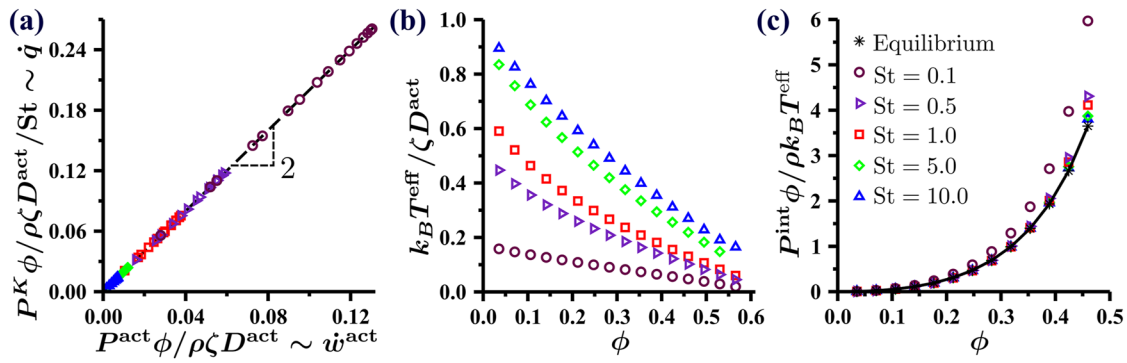

FIG. 3. Active Brownian spheres with $\ell_0/\sigma = 5.0$ and in the homogeneous fluid state. (a) Parametric plot of heat and work production for all ϕ and St examined [see legend in panel (c)]. Dependence of (b) $k_B T^{\text{eff}}$ and (c) P^{int} (normalized by $k_B T^{\text{eff}}$) on ϕ and St.

Published under an exclusive license by AIP Publishing

only the tails of the distribution are appreciably altered as significant changes to the distribution would likely be reflected in the equation of state [see Fig. 3(c)].

CONCLUSIONS

Despite strictly violating the FDT, translational active forces can result in particle distributions that appear to admit effective equilibrium states in the limit of large translational inertia. We note that *rotational* inertia, in the case of ABPs, has been recently reported to accentuate MIPS by increasing the effective persistence length of particle trajectories.[49,81] We thus emphasize that it is only in the limit of large *translational* inertia that active phase transitions caused by *translational* active forces are mitigated. It would be interesting to examine the role of rotational inertia in the structures generated by chiral active matter.[82] This limit can be rigorously understood in the absence of interactions, where the conversion of nonequilibrium active stress to kinetic stress renders the density distribution to be Boltzmann with the kinetic temperature serving as an effective temperature. For the interacting systems we have studied, this limit eliminates nonequilibrium phase transitions while restoring equilibrium-like transitions. However, a key distinction of this limit from true equilibrium is the concentration dependence of the effective temperature, which leads to deviations from the anticipated equilibrium behavior. While we have focused most of our attention on athermal systems, it is interesting to consider scenarios in which active systems are in contact with an equilibrium bath with a temperature of k_BT. In the high inertia limit, the temperature of the particles will be $k_B(T^{\text{eff}}(\phi) + T)$. For the systems examined here, $k_BT^{\text{eff}}(\phi)$ is a monotonically decreasing function of density, and it can thus be expected that in the high density limit, the system will be *truly in equilibrium* with a temperature of k_BT as $T \gg T^{\text{eff}}(\phi)$. Finally, it remains to be seen if, by constructing an equation of state for $k_BT^{\text{eff}}(\phi)$, the familiar tools of thermodynamics may be used to understand phase transitions of active systems in the large inertia limit. Such a framework would provide a powerful tool for understanding and tuning the phase behavior of driven systems. In the absence of a thermodynamic framework, a recently proposed mechanical theory of nonequilibrium coexistence may be used to describe inertial phase behavior.[66]

SUPPLEMENTARY MATERIAL

See the supplementary material, which includes Refs. 9, 38, 46, 57, 58, 61, 62, 83, and 84, for derivation and discussion of the distribution of ideal inertial ABPs, simulation and phase diagram construction details, and additional equation-of-state data for interacting ABPs in 3D.

ACKNOWLEDGMENTS

We dedicate this paper to the memory of our late friend, colleague, and mentor, Phill Geissler.

We acknowledge helpful discussions with Cory Hargus, Kranthi Mandadapu, and Keith Burnett. P.L.G. was supported by the U.S. Department of Energy, Office of Basic Energy Sciences, through the Chemical Sciences Division (CSD) of Lawrence Berkeley National Laboratory (LBNL), under Contract No. DE-AC02-05CH11231. J.F.B. acknowledges support by the National Science Foundation under Grant No. CBET-1803662. We gratefully acknowledge the support of the NVIDIA Corporation for the donation of the Titan V GPU used to carry out part of this work.

AUTHOR DECLARATIONS

Conflict of Interest

The authors have no conflicts to disclose.

Author Contributions

Ahmad K. Omar: Conceptualization (equal); Writing – original draft (equal); Writing – review & editing (equal). **Katherine Klymko**: Conceptualization (equal); Writing – original draft (equal); Writing – review & editing (equal). **Trevor GrandPre**: Conceptualization (equal); Writing – original draft (equal); Writing – review & editing (equal). **Phillip L. Geissler**: Conceptualization (equal); Writing – original draft (equal); Writing – review & editing (equal). **John F. Brady**: Conceptualization (equal); Writing – original draft (equal); Writing – review & editing (equal).

DATA AVAILABILITY

The data that support the findings of this study are available from the corresponding author upon reasonable request.

REFERENCES

[1] Y. Fily and M. C. Marchetti, Phys. Rev. Lett. **108**, 235702 (2012).
[2] G. S. Redner, M. F. Hagan, and A. Baskaran, Phys. Rev. Lett. **110**, 055701 (2013).
[3] I. Buttinoni, J. Bialké, F. Kümmel, H. Löwen, C. Bechinger, and T. Speck, Phys. Rev. Lett. **110**, 238301 (2013).
[4] M. E. Cates and J. Tailleur, Annu. Rev. Condens. Matter Phys. **6**, 219 (2015).
[5] J. Dzubiella, G. P. Hoffmann, and H. Löwen, Phys. Rev. E **65**, 021402 (2002).
[6] T. Vissers, A. Wysocki, M. Rex, H. Löwen, C. P. Royall, A. Imhof, and A. van Blaaderen, Soft Matter **7**, 2352 (2011).
[7] K. Klymko, P. L. Geissler, and S. Whitelam, Phys. Rev. E **94**, 022608 (2016).
[8] M. Han, J. Yan, S. Granick, and E. Luijten, Proc. Natl. Acad. Sci. U. S. A. **114**, 7513 (2017).
[9] C. del Junco, L. Tociu, and S. Vaikuntanathan, Proc. Natl. Acad. Sci. U. S. A. **115**, 3569 (2018).
[10] C. del Junco and S. Vaikuntanathan, J. Chem. Phys. **150**, 094708 (2019).
[11] L. F. Cugliandolo, J. Phys. A: Math. Theor. **44**, 483001 (2011).
[12] S. F. Edwards and R. B. S. Oakeshott, Physica A **157**, 1080 (1989).
[13] A. Mehta and S. F. Edwards, Physica A **157**, 1091 (1989).
[14] I. K. Ono, C. S. O'Hern, D. J. Durian, S. A. Langer, A. J. Liu, and S. R. Nagel, Phys. Rev. Lett. **89**, 095703 (2002).
[15] C. S. O'Hern, A. J. Liu, and S. R. Nagel, Phys. Rev. Lett. **93**, 165702 (2004).
[16] T. F. F. Farage, P. Krinninger, and J. M. Brader, Phys. Rev. E **91**, 042310 (2015).
[17] S. C. Takatori and J. F. Brady, Phys. Rev. E **91**, 032117 (2015).
[18] M. Rein and T. Speck, Eur. Phys. J. E **39**, 84 (2016).
[19] R. Wittmann and J. M. Brader, Europhys. Lett. **114**, 68004 (2016).
[20] R. Wittmann, C. Maggi, A. Sharma, A. Scacchi, J. M. Brader, and U. Marini Bettolo Marconi, J. Stat. Mech.: Theory Exp. **2017**, 113207.
[21] R. Wittmann, U. Marini Bettolo Marconi, C. Maggi, and J. M. Brader, J. Stat. Mech.: Theory Exp. **2017**, 113208.
[22] R. Wittmann, F. Smallenburg, and J. M. Brader, J. Chem. Phys. **150**, 174908 (2019).

Published under an exclusive license by AIP Publishing

[23]F. Turci and N. B. Wilding, Phys. Rev. Lett. **126**, 038002 (2021).
[24]D. Loi, S. Mossa, and L. F. Cugliandolo, Phys. Rev. E **77**, 051111 (2008).
[25]J. Palacci, C. Cottin-Bizonne, C. Ybert, and L. Bocquet, Phys. Rev. Lett. **105**, 088304 (2010).
[26]S. Wang and P. G. Wolynes, J. Chem. Phys. **135**, 051101 (2011).
[27]D. Loi, S. Mossa, and L. F. Cugliandolo, Soft Matter **7**, 10193 (2011).
[28]K. I. Morozov and L. M. Pismen, Phys. Rev. E **81**, 061922 (2010).
[29]G. Szamel, Phys. Rev. E **90**, 012111 (2014).
[30]A. P. Solon, M. E. Cates, and J. Tailleur, Eur. Phys. J. Spec. Top. **224**, 1231 (2015).
[31]S. C. Takatori, R. De Dier, J. Vermant, and J. F. Brady, Nat. Commun. **7**, 10694 (2016).
[32]T. GrandPre and D. T. Limmer, Phys. Rev. E **98**, 060601(R) (2018).
[33]E. W. Burkholder and J. F. Brady, J. Chem. Phys. **150**, 184901 (2019).
[34]J. O'Byrne and J. Tailleur, Phys. Rev. Lett. **125**, 208003 (2020).
[35]J. O'Byrne, Y. Kafri, J. Tailleur, and F. van Wijland, Nat. Rev. Phys. **4**, 167–183 (2022).
[36]É. Fodor, C. Nardini, M. E. Cates, J. Tailleur, P. Visco, and F. van Wijland, Phys. Rev. Lett. **117**, 038103 (2016).
[37]D. Mandal, K. Klymko, and M. R. DeWeese, Phys. Rev. Lett. **119**, 258001 (2017).
[38]A. K. Omar, K. Klymko, T. GrandPre, and P. L. Geissler, Phys. Rev. Lett. **126**, 188002 (2021).
[39]S. Mandal, B. Liebchen, and H. Löwen, Phys. Rev. Lett. **123**, 228001 (2019).
[40]Q.-L. Lei and R. Ni, Proc. Natl. Acad. Sci. U. S. A. **116**, 22983 (2019).
[41]C. Dai, I. R. Bruss, and S. C. Glotzer, Soft Matter **16**, 2847 (2020).
[42]J.-j. Liao, F.-j. Lin, and B.-q. Ai, Physica A **582**, 126251 (2021).
[43]G. Negro, C. B. Caporusso, P. Digregorio, G. Gonnella, A. Lamura, and A. Suma, Eur. Phys. J. E **45**, 75 (2022).
[44]A. Attanasi, A. Cavagna, L. Del Castello, I. Giardina, T. S. Grigera, A. Jelić, S. Melillo, L. Parisi, O. Pohl, E. Shen, and M. Viale, Nat. Phys. **10**, 691 (2014).
[45]A. Manacorda and A. Puglisi, Phys. Rev. Lett. **119**, 208003 (2017).
[46]S. C. Takatori and J. F. Brady, Phys. Rev. Fluids **2**, 094305 (2017).
[47]C. Scholz, S. Jahanshahi, A. Ldov, and H. Löwen, Nat. Commun. **9**, 5158 (2018).
[48]H. Löwen, J. Chem. Phys. **152**, 040901 (2020).
[49]M. Sandoval, Phys. Rev. E **101**, 012606 (2020).
[50]L. Caprini and U. M. B. Marconi, J. Chem. Phys. **154**, 024902 (2021).
[51]J. Su, H. Jiang, and Z. Hou, New J. Phys. **23**, 013005 (2021).
[52]A. R. Sprenger, S. Jahanshahi, A. V. Ivlev, and H. Löwen, Phys. Rev. E **103**, 042601 (2021).
[53]R. Chatterjee, N. Rana, R. A. Simha, P. Perlekar, and S. Ramaswamy, Phys. Rev. X **11**, 031063 (2021).
[54]M. te Vrugt, J. Jeggle, and R. Wittkowski, New J. Phys. **23**, 063023 (2021).
[55]J. Mayer Martins and R. Wittkowski, Phys. Rev. E **106**, 034616 (2022).
[56]M. te Vrugt, T. Frohoff-Hülsmann, E. Heifetz, U. Thiele, and R. Wittkowski, arXiv:2204.03018 (2022).
[57]S. Plimpton, J. Comput. Phys. **117**, 1 (1995).
[58]J. A. Anderson, J. Glaser, and S. C. Glotzer, Comput. Mater. Sci. **173**, 109363 (2020).
[59]W. G. Hoover and F. H. Ree, J. Chem. Phys. **49**, 3609 (1968).
[60]P. N. Pusey, E. Zaccarelli, C. Valeriani, E. Sanz, W. C. K. Poon, and M. E. Cates, Philos. Trans. R. Soc. A **367**, 4993 (2009).
[61]H. Risken, *The Fokker-Planck Equation*, 2nd ed. (Springer-Verlag, Berlin, 1989).
[62]W. Yan and J. F. Brady, J. Fluid Mech. **785**, R1 (2015).
[63]J. Rodenburg, M. Dijkstra, and R. Van Roij, Soft Matter **13**, 8957 (2017).
[64]J. M. Epstein, K. Klymko, and K. K. Mandadapu, J. Chem. Phys. **150**, 164111 (2019).
[65]A. K. Omar, Z.-G. Wang, and J. F. Brady, Phys. Rev. E **101**, 012604 (2020).
[66]A. K. Omar, H. Row, S. A. Mallory, and J. F. Brady, arXiv:2211.12673 (2022).
[67]S. A. Mallory, A. Šarić, C. Valeriani, and A. Cacciuto, Phys. Rev. E **89**, 052303 (2014).
[68]Y. Fily, S. Henkes, and M. C. Marchetti, Soft Matter **10**, 2132 (2014).
[69]S. C. Takatori, W. Yan, and J. F. Brady, Phys. Rev. Lett. **113**, 028103 (2014).
[70]A. P. Solon, J. Stenhammar, R. Wittkowski, M. Kardar, Y. Kafri, M. E. Cates, and J. Tailleur, Phys. Rev. Lett. **114**, 198301 (2015).
[71]A. P. Solon, Y. Fily, A. Baskaran, M. E. Cates, Y. Kafri, M. Kardar, and J. Tailleur, Nat. Phys. **11**, 673 (2015).
[72]S. Paliwal, J. Rodenburg, R. van Roij, and M. Dijkstra, New J. Phys. **20**, 015003 (2018).
[73]S. Shankar and M. C. Marchetti, Phys. Rev. E **98**, 020604(R) (2018).
[74]T. Nemoto, É. Fodor, M. E. Cates, R. L. Jack, and J. Tailleur, Phys. Rev. E **99**, 022605 (2019).
[75]L. Tociu, É. Fodor, T. Nemoto, and S. Vaikuntanathan, Phys. Rev. X **9**, 041026 (2019).
[76]É. Fodor, T. Nemoto, and S. Vaikuntanathan, New J. Phys. **22**, 013052 (2020).
[77]T. GrandPre, K. Klymko, K. K. Mandadapu, and D. T. Limmer, Phys. Rev. E **103**, 012613 (2021).
[78]Y.-E. Keta, É. Fodor, F. van Wijland, M. E. Cates, and R. L. Jack, Phys. Rev. E **103**, 022603 (2021).
[79]K. Goswami, Phys. Rev. E **105**, 044123 (2022).
[80]N. H. Nguyen, D. Klotsa, M. Engel, and S. C. Glotzer, Phys. Rev. Lett. **112**, 075701 (2014).
[81]E. A. Lisin, O. S. Vaulina, I. I. Lisina, and O. F. Petrov, Phys. Chem. Chem. Phys. **24**, 14150 (2022).
[82]B. Zhang and A. Snezhko, Phys. Rev. Lett. **128**, 218002 (2022).
[83]J. D. Weeks, D. Chandler, and H. C. Andersen, J. Chem. Phys. **54**, 5237 (1971).
[84]P. J. Steinhardt, D. R. Nelson, and M. Ronchetti, Phys. Rev. B **28**, 784 (1983).

Published under an exclusive license by AIP Publishing